online data

Controlled alteration of the shape and conformational stability of α-helical cell-lytic peptides: effect on mode of action and cell specificity

Igor ZELEZETSKY*, Sabrina PACOR†, Ulrike PAG‡, Niv PAPO§, Yechiel SHAI§, Hans-Georg SAHL‡ and Alessandro TOSSI*[1]

*Department of Biochemistry, Biophysics and Macromolecular Chemistry, University of Trieste, I-34127 Trieste, Italy, †Department of Biomedical Sciences, University of Trieste, I-34127 Trieste, Italy, ‡Institute for Medical Microbiology and Immunology, University of Bonn, 53105 Bonn, Germany, and §Department of Biological Chemistry, Weizmann Institute of Science, Rehovot 76100, Israel

A novel method, based on the rational and systematic modulation of macroscopic structural characteristics on a template originating from a large number of natural, cell-lytic, amphipathic α-helical peptides, was used to probe how the depths and shapes of hydrophobic and polar faces and the conformational stability affect antimicrobial activity and selectivity with respect to eukaryotic cells. A plausible mode of action explaining the peptides' behaviour in model membranes, bacteria and host cells is proposed. Cytotoxic activity, in general, correlated strongly with the hydrophobic sector depth, and required a majority of aliphatic residue side chains having more than two carbon atoms. It also correlated significantly with the size of polar sector residues, which determines the penetration depth of the peptide via the so-called snorkel effect. Both an oblique gradient of long to short aliphatic residues along the hydrophobic face and a stabilized helical structure increased activity against host cells but not against bacteria, as revealed by haemolysis, flow cytofluorimetric studies on lymphocytes and surface plasmon resonance studies with model phosphatidylcholine/cholesterol membranes. The mode of interaction changes radically for a peptide with a stable, preformed helical conformation compared with others that form a structure only on membrane binding. The close correlation between effects observed in biological and model systems suggests that the 'carpet model' correctly represents the type of peptides that are bacteria-selective, whereas the behaviour of those that lyse host cells is more complex.

Key words: amphipathic helix, antimicrobial peptide, cell specificity, cell-lytic peptide, mode of action, surface plasmon resonance.

INTRODUCTION

Peptide–membrane interactions are essential for many processes of physiological or pathological relevance, such as the effects of hormones or toxins on host cells or the effects of host defence peptides on microbial cells [1–3]. The mode of action of cytotoxic peptides can indicate new design strategies for the development of therapeutic agents, such as immunotoxins [4], antitumour drugs [5] or anti-infective agents capable of overcoming the currently serious problem of resistance to conventional antibiotics [6]. For AMPs (antimicrobial peptides), activity depends principally on membrane permeabilization or lysis, and several mechanisms of action have been proposed, ranging from the formation of highly organized transmembrane pores, to more dynamic supramolecular peptide–lipid complexes leading to toroidal or wormhole-type pores, to a relatively disorganized, detergent-like membrane disaggregation due to hydrophobic and/or electrostatic interactions with the membrane surface [7–11]. However, the molecular details underlying these processes, which have important implications for the selectivity of the peptides' activity, are still not entirely understood.

One important class of membrane-interacting peptides assume an amphipathic α-helical conformation that permits the insertion of a well-defined hydrophobic sector into the lipid bilayer [8]. We have undertaken a systematic study of how the structural and physical characteristics of these peptides influence the mode and selectivity of their membranolytic action by rationally and independently varying properties such as charge, hydrophobicity, amphipathicity and helix-forming propensity [8,12–14]. To do this, we have used a self-consistent set of peptides of fixed size, whose design is based on a sequence template obtained from the comparative analysis of the sequences from numerous natural antimicrobial and/or cytotoxic peptides of different origins [8,13]. Thus these peptides are based on a scaffold that has been selected by evolution in many different organisms, whereas the precise sequence has been rationally adapted to probe the role of specific aspects of the molecules' shape and stability. Previous studies have indicated that the helix-forming propensity is a key factor in determining selectivity, i.e. the differential cytotoxicity towards bacterial or host cell membranes, whereas the properties of the hydrophobic and polar sector can influence both host cell cytotoxicity and antimicrobial potency [13,15].

The roles of helical structuring and hydrophobic face properties in determining membrane interaction are intimately related. Helix formation permits an optimal spatial arrangement of aliphatic side chains for membrane insertion. The strong hydrophobic interaction of these side chains with the lipid layer, in turn, stabilizes the helical conformation, reducing main-chain hydrophobicity and thus allowing a deeper insertion into the bilayer. To probe these interrelationships, we have designed a new set of peptides in which the size, cationicity and the amphipathic residue arrangement were not varied, whereas (i) the size of aliphatic side chains for residues forming the hydrophobic surface of the helix was systematically varied to determine the minimum

Abbreviations used: Abu, 2-aminobutyric acid; Acp, aminocylcopentanecarboxylic acid; Aib, 2-aminoisobutyric acid; AMP, antimicrobial peptide; Dab, 2,4-diaminobutyric acid; Dap, 2,3-diaminopropionic acid; Deg, diethylglycine; Dpg, dipropylglycine; FS, forward scattering; Hse, homoserine; MH, Mueller–Hinton; MIC, minimum inhibitory concentration; Nle, norleucine; Nva, norvaline; ONPG, *o*-nitrophenyl β-D-galactopyranoside; PC, phosphatidylcholine; PE, phosphatidylethanolamine; PG, phosphatidylglycerol; PI, propidium iodide; SEM, scanning electron microscopy; SPR, surface plasmon resonance; SS, side scattering; TFE, trifluoroethanol.

[1] To whom correspondence should be addressed (email tossi@bbcm.units.it).

Table 1 Sequences of synthesized model peptides, based on a template derived from natural α-helical AMPs

Peptide*	Sequence	Molecular mass (Da)	
		Calculated	Measured†
P1	Gly-Nle-Nle-Gln-Gln-Nle-Gly-Orn-Orn-Nle-Orn-Gln-Nle-Nle-Gln-Orn-Nle-Gly-Tyr	2112.6	2113.2
P2	Gly-Nle-Nle-Gln-Gln-Nle-Aib-Orn-Orn-Aib-Orn-Gln-Aib-Nle-Gln-Orn-Nle-Gly-Tyr	2084.6	2085.2
P3	Gly-Nle-Nle-Gln-Gln-Nle-Acp-Orn-Orn-Acp-Orn-Gln-Acp-Nle-Gln-Orn-Nle-Gly-Tyr	2162.7	2163.2
P4	Gly-Abu-Abu-Gln-Gln-Abu-Deg-Orn-Orn-Deg-Orn-Gln-Deg-Abu-Gln-Orn-Abu-Gly-Tyr	2028.5	2028.0
P5	Gly-Abu-Abu-Gln-Gln-Abu-Aib-Orn-Orn-Aib-Orn-Gln-Aib-Abu-Gln-Orn-Abu-Gly-Tyr	1944.3	1944.4
P6	Gly-Nva-Nva-Asn-Asn-Nva-Dpg-Orn-Orn-Dpg-Orn-Asn-Dpg-Nva-Asn-Orn-Nva-Gly-Tyr	2126.6	2126.4
P7	Gly-Nle-Nle-Gln-Gln-Nle-Aib-Lys-Lys-Aib-Lys-Gln-Aib-Nle-Gln-Lys-Nle-Gly-Tyr	2140.7	2140.4
P8	Gly-Nle-Nle-Hse-Hse-Nle-Aib-Dab-Dab-Aib-Dab-Hse-Aib-Nle-Hse-Dab-Nle-Gly-Tyr	1920.3	1920.0
P9	Gly-Nle-Nle-Ser-Ser-Nle-Aib-Dap-Dap-Aib-Dap-Ser-Aib-Nle-Ser-Dap-Nle-Gly-Tyr	1808.1	1808.0
P10	Gly-Nle-Nle-Gln-Gln-Nva-Acp-Orn-Orn-Deg-Orn-Gln-Aib-Abu-Gln-Orn-Ala-Gly-Tyr	2054.5	2054.0
P11	Gly-Ala-Abu-Gln-Gln-Nva-Aib-Orn-Orn-Deg-Orn-Gln-Acp-Nle-Gln-Orn-Nle-Gly-Tyr	2054.5	2054.0

* P1 and P2 also termed as P19(5) and P19(5|B) respectively in [8,13].
† Mass error $\leqslant$ 0.3 Da.

requirements for interaction with different types of cells, leading to membrane lysis; (ii) the shape of the hydrophobic surface was modulated to test whether an oblique hydrophobic gradient could affect membrane insertion and selectivity; (iii) the size of side chains for residues forming the polar surface of the helix was varied to determine how the degree of insertion of the peptide via the so-called snorkel effect affected activity; and (iv) the helix-forming propensity was independently varied to probe the role of helix stability in modulating selectivity. Although the literature on structure–activity relationships in α-helical cell-lytic peptides is vast [8,16–20], our method, which is based on the rational and systematic modulation of macroscopic structural characteristics on a template originating from a large number of cell-lytic natural peptides, is unique.

The capacity of the peptides to compromise microbial cells was assessed in terms of MIC (minimum inhibitory concentration) values towards a number of laboratory microbial strains and of the kinetics for bacterial killing and membrane permeabilization in reference Gram-positive and Gram-negative microorganisms. Flow cytometric techniques were used to correlate permeabilization of circulating blood cells with morphological changes, which could also be visualized by SEM (scanning electron microscopy). Furthermore, a plasmon resonance technique was used to assess the mode of interaction with both anionic- and zwitterionic-model lipid bilayers. Finally, the activity of the most active peptides was assessed for a wide panel of indicator microbial strains, including several Gram-positive, Gram-negative and fungal clinical isolates, some of which are multi-resistant to conventional antibiotics. The wide-spectrum and potent activity of some of the peptides indicate that they may be suitable lead compounds for the development of novel anti-infective agents.

MATERIALS AND METHODS

Chemicals

PEG-PS [poly(ethylene glycol)-polystyrene] resin and HATU [*O*-(7-azabenzotriazol-1-yl)-1,1,3,3-tetramethyluronium hexafluorophosphate] were obtained from Applied Biosystems (Forster City, CA, U.S.A.), TBTU [*O*-(benzotriazol-1-yl)-1,1,3,3-tetramethyluronium tetrafluoroborate] and Fmoc (fluoren-9-ylmethoxycarbonyl)-protected amino acids were obtained from Applied Biotech Italy (Milan, Italy). All other reagents and solvents used were of synthesis grade. MH (Mueller–Hinton) broth and Bacto-agar were obtained from Difco (Detroit, MI, U.S.A.), ONPG (*o*-nitrophenyl β-D-galactopyranoside), egg PC (phosphatidylcholine), egg PG (phosphatidylglycerol), type V PE (phosphatidylethanolamine) from *Escherichia coli*, OG (*N*-octyl β-D-glucopyranoside) and BSA were obtained from Sigma (St. Louis, MO, U.S.A.), CENTA was obtained from Calbiochem (Darmstadt, Germany), and Dulbecco's modified Eagle's medium and foetal bovine serum were from Celbio (Milan, Italy). Cholesterol (extra pure) was supplied by Merck (Darmstadt, Germany). All other reagents were of analytical grade. Buffers were prepared in double glass-distilled water.

Peptide design, synthesis and characterization

Peptide design and physicochemical properties

Peptides were designed using a previously reported sequence template, obtained by analysing the frequency of different types of amino acid at each of the first 18 positions in over 150 natural host defence or cytotoxic peptides [8,12,13]. For this study, the template was filled using both proteinogenic and non-proteinogenic amino acids selected for appropriate side-chain characteristics, and the resulting sequences are shown in Table 1, whereas helical wheel projections are shown in Figures 1 and 2.

The amino acid hydrophobicity index scale used for determining the mean hydrophobicity and amphipathicity per residue of these peptides (Table 2) was developed *ad hoc* as a normalized and filtered consensus of 163 published scales [21], and is arbitrarily ranged between values of $+10$ for Phe and -10 for Arg. For more details, see the Supplementary Materials and methods section at http://www.BiochemJ.org/bj/390/bj3900177add.htm.

Peptide synthesis and characterization

Automated solid phase peptide syntheses were performed with the column thermostatically maintained at 50 °C and loaded with PEG-PS resin (substitution 0.17–0.22 mmol/g) for all peptides but the one containing Dpg (dipropylglycine) was synthesized manually. Peptides were purified by preparative RP-HPLC [Waters Delta-Pak® C_{18}, 15 μm, 300 Å (1 Å = 0.1 nm), 25 mm × 100 mm], followed by electrospray ionization MS determination and spectrophotometric quantification. CD spectra were obtained on a Jasco J-715 spectropolarimeter and the helix content was determined using the measured ellipticity at 222 nm. Details are provided in the Supplementary Materials and methods section at http://www.BiochemJ.org/bj/390/bj3900177add.htm.

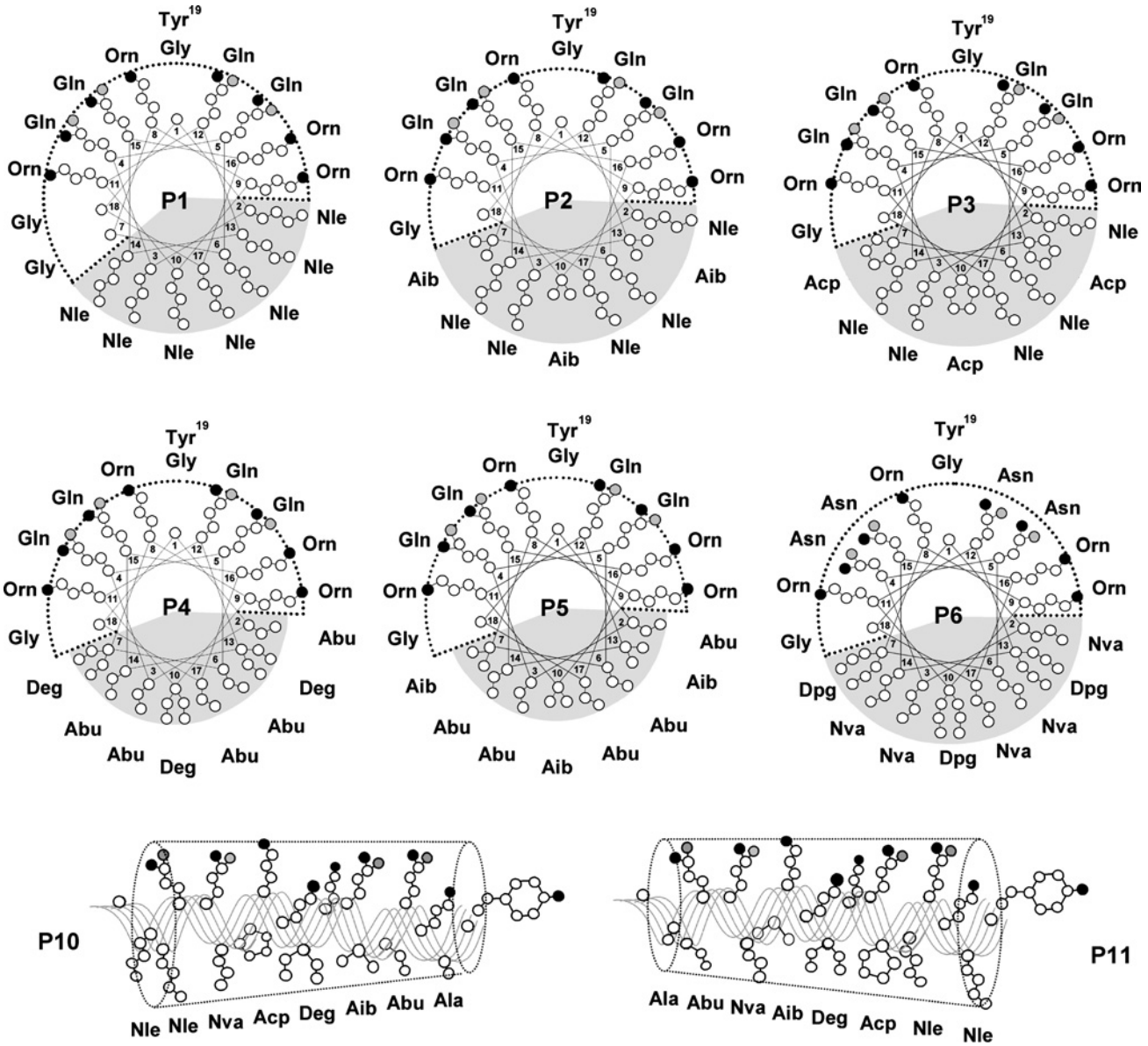

Figure 1 Helical wheel projections for model peptides with altered hydrophobic face

Residue side-chain structures are shown schematically with atoms as circles, including the α-carbon atom (white for carbon, grey for oxygen and black for nitrogen). P1 is the parent peptide and the polar sector is indicated by a dotted frame, while the hydrophobic face by grey shading. This is increasingly shallower in P4 and P5, less dense in long side chains in P2, more dense in long side chains in P6 and shows an N → C-terminal or C → N-terminal depth gradient in P10 and P11. The α-branched residues in P2 and P3 increasingly stabilize the helical conformation. The three-letter non-proteinogenic residue nomenclature is explained in the text.

Membrane binding studies

SPR (surface plasmon resonance)

Small unilamellar vesicles were prepared by sonication of PC/cholesterol (10:1, w/w) or PE/PG (7:3, w/w) dispersions as described previously [22], and determined to be unilamellar with an average diameter of 20–50 nm using a JEOL JEM 100B electron microscope (Japan Electron Optics Laboratory, Tokyo, Japan). Biosensor experiments were performed with a BIAcore 3000 analytical system (BIAcore, Uppsala, Sweden) using an L1 sensor chip (BIAcore) whose surface consists of a dextran matrix modified with lipophilic compounds that capture small unilamellar vesicles, permitting the retention of a bilayer structure [23]. Experiments were always performed at 25 °C with PBS as the running buffer, as described in the Supplementary Materials and methods section at http://www.BiochemJ.org/bj/390/bj3900177add.htm.

The peptide–lipid binding event was analysed using a series of sensograms collected at six different peptide concentrations. As the system did not reach steady state during the injection of the sample, the affinity constant was determined using kinetic models suitable for peptide–lipid interactions, by curve fitting using numerical integration analysis (see the Supplementary Materials and methods section at http://www.BiochemJ.org/bj/390/bj3900177add.htm). The BIA evaluation software offers different reaction models to perform complete kinetic analyses of the peptide sensograms. One curve-fitting algorithm (the two-state reaction model) was chosen on the basis of what was known about the possible binding mechanisms of lytic peptides. The data were treated globally by simultaneously fitting the peptide sensograms

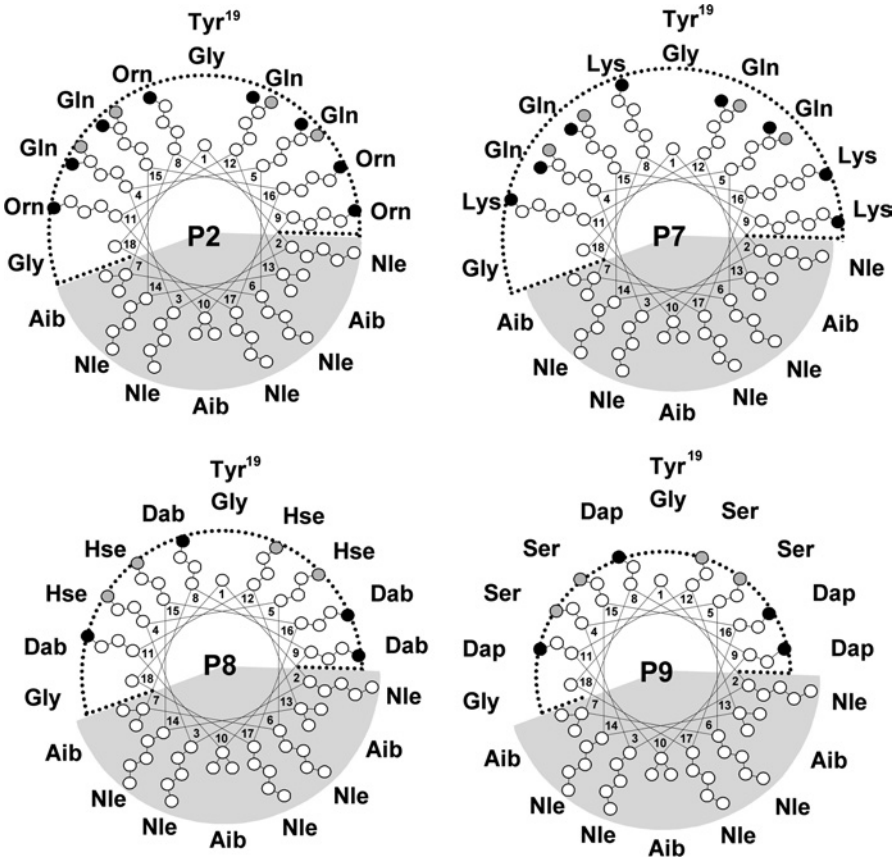

Figure 2 Helical wheel projections for model peptides with altered polar face

Residue side-chain structures are shown schematically with atoms as circles (white for carbon, grey for oxygen and black for nitrogen). The hydrophobic face is that of P2 while the depth of the polar sector is indicatively shown by a dotted frame. For the three-letter non-proteinogenic residue nomenclature, see the text.

obtained at the six different concentrations. The two-state reaction model [23] was applied to each dataset corresponding to the following model:

$$P + L \underset{k_{d1}}{\overset{k_{a1}}{\rightleftharpoons}} PL \underset{k_{d2}}{\overset{k_{a2}}{\rightleftharpoons}} PL^*$$

where the peptide (P)–lipid (L) interaction of the first step (PL) corresponds to surface binding and leads to PL^* in the second step, corresponding to partial insertion of the peptide into the lipid bilayer, where it cannot dissociate directly to $P + L$ (see the Supplementary Materials and methods section for differential equations at http://www.BiochemJ.org/bj/390/bj3900177add.htm).

Biological activity assays

Antimicrobial activity assays

The bacteriostatic activity of all the synthetic peptides on standard laboratory strains was determined as an MIC by a microdilution susceptibility test as described previously [12,14], starting with 32 μM peptide and using 10^5 c.f.u./ml (where c.f.u. stands for colony-forming units) microorganisms in the exponential phase. The MIC was considered to correspond to the first well without visible growth after overnight incubation at 37 °C. For selected active peptides, MIC values were determined under more stringent conditions as described in the Supplementary Materials and methods section at http://www.BiochemJ.org/bj/390/bj3900177add.htm.

The permeabilization of the cytoplasmic membranes of *E. coli* ML-35 and of *Staphylococcus aureus* 710A, by synthetic peptides, was evaluated by following the unmasking of cytoplasmic β-galactosidase and phosphogalactosidase activities respectively to extracellular ONPG (Sigma, St. Louis, MO, U.S.A.) or ONPG-6-phosphate, as described previously [24] and in more details in the Supplementary Materials and methods section at http://www.BiochemJ.org/bj/390/bj3900177add.htm. Unmasking of periplasmic β-lactamase activity to CENTA was used to follow the Gram-negative outer-membrane permeabilization.

The bactericidal activity was tested against *E. coli* ML-35 or *Staph. aureus* 710A in the exponential phase (10^7 c.f.u./ml in PBS incubated at 37 °C). At different times, 50 μl of the bacteria/peptide suspension was diluted severalfold in ice-cold PBS, and the solution was plated on nutrient agar and incubated for 16–18 h to allow colony counts.

Haemolytic activity

Lysis of erythrocyte membranes was determined by monitoring the release of haemoglobin at 415 nm, from 0.5 % human erythrocyte suspensions (0.2 ml) in relation to complete (100 %) haemolysis as determined by the addition of 0.2 % Triton X-100.

Flow cytometric analyses

Suspensions of 10^6 lymphocytes (see the Supplementary Materials and methods section for preparation at http://www.BiochemJ.org/bj/390/bj3900177add.htm) in 1 ml of PBS were

Table 2 Correlation between peptide physicochemical properties and antimicrobial or haemolytic activity

Peptide	P1	P2	P3	P4	P5	P6	P7	P8	P9	P10	P11
Structural and physical properties											
Mean hydrophobicity*	−0.06	−0.70	0.09	−1.80	−2.65	0.04	−0.90	−0.25	−0.45	−1.30	−1.30
Relative amphipathicity*	0.66	0.56	0.64	0.43	0.34	0.67	0.57	0.50	0.53	0.47	0.53
% helicity† (water)	5	10	60	<5	5	10	25	10	5	10	10
% helicity (50% TFE)	60	75	100	60	40	35	90	90	90	45	45
% helicity (10 mM SDS)	65	80	100	65	45	35	95	90	60	50	40
Retention time (min)‡	23.7	22.9	25.3	17.9	15.1	24.1	23.5	22.2	19.9	20.9	20.5
Antimicrobial activity (MIC, μM)§											
E. coli (ML-35)	1	1 (1)	8 (0.5)	16	>32	2	1	1	2	8	8
Ps. aeruginosa (ATCC 27853)	1	2	16 (0.5)	>32	>32	2	0.5	1	4	32	>32
Salmonella typhimurium (ATCC 14028)	2	1	16 (1)	>32	>32	4	1–2	2	16	16–32	32
Staph. aureus (710A)	4	2–4 (2)	4–8 (1)	>32	>32	2	1	1	4	>32 (16)	>32 (16)
Bacillus megaterium (BM11)	1–2	1	4 (0.5–1)	>32	>32	4	1	1	4	8	8
C. albicans (c.i.)	8	8	4	>32	>32	>32	16	16	>32	>32	>32
Bacterial membrane permeabilization‖											
E. coli (outer)	++	+++	+++	−	−	+++	+++	++	+	+	++
E. coli (cytoplasmic)	++	++	+++	−	−	+++	++	++	+	+	++
Staph. aureus (cytoplasmic)	++	++	++	−	−	+++	++	+	+	−	−
Haemolytic activity (% lysis)¶											
10 μM peptide	10±5	10±5	>95	<5	<5	25	25±5	25±5	15±10	20±5	20±5
100 μM peptide	60±15	55±10	>95	15±5	<5	90±10	90±10	55±15	30±7	85±5	85±5

* Mean hydrophobicity per residue (H) and hydrophobic moment relative to that of a maximally amphipathic peptide ($\mu H/\mu H_{max}$).

† CD spectra of the selected peptides are provided in Figure S1.

‡ RP-HPLC under fixed gradient conditions.

§ Mean for three independent trials run in duplicate in 50% MH broth in PBS or, in parentheses, in 5% MH broth in PBS.

‖ Qualitative bacterial permeabilization kinetics scores were assigned on the basis of data from permeabilization plots (see Figure S2), in the presence of 5 μM peptide (+++, very fast; ++, fast; +, slow; −, not active).

¶ Mean for two independent trials, run in duplicate, with a 0.5% erythrocyte suspension in PBS.

exposed to 0.01–10 μM of the desired peptide for 30 min at 37 °C. The reaction was stopped by centrifugation at 400 ***g*** for 5 min at 4 °C followed by a double washing with PBS, resuspension and then addition of 10 μl of PI (propidium iodide) solution (0.5 mg/ml in PBS) immediately before flow cytometric analysis. Five samples for each peptide solution were prepared. Fluorescence data from damaged cells showing permeability to PI was acquired in a monoparametric histogram (emission wavelength, 612 nm), using an XL instrument (Coulter, Miami, FL, U.S.A.). At least 10000 events were acquired for each sample. Histograms were analysed with the WinMDI software (Dr J. Trotter, Scripps Research Institute, La Jolla, CA, U.S.A.). Cytometric data were submitted to computer-assisted analysis using the Student–Newman–Keuls test of variance. Morphological changes observed by flow cytometry were compared with those observed by SEM, using appropriately treated lymphocytes as described in the Supplementary Materials and methods section at http://www.BiochemJ.org/bj/390/bj3900177add.htm.

RESULTS

Peptide design and structural characteristics

The parent sequence (here termed P1, net charge +5, see Table 1 and Figure 1) was obtained previously [13] by filling out a sequence template with Nle (norleucine), Gln and Orn, all having linear side chains of four carbon atoms, arranged to form a markedly amphipathic helix. It was bracketed by Gly in positions 1 and 18, while Gly in position 7 (as present in ~30% of natural peptides) seems to reduce the cytotoxicity to host cells. A C-terminal Tyr was added for accurate quantification. P1 had been found to combine a rapid, broad-spectrum antimicrobial activity with a moderately low haemolytic activity [13].

In the series P2–P6, the depth of the hydrophobic face was systematically varied by reducing the size of the aliphatic side chain from 4 to 1 carbon atoms one at a time, by replacing Nle with Nva (norvaline), Abu (2-aminobutyric acid) or Ala (see Table 1 and Figure 1). Furthermore, achiral, α-branched residues with side chains varying from 3 to 1 carbon atoms [Dpg, its cyclic analogue Acp (aminocylcopentanecarboxylic acid), Deg (diethylglycine) or Aib (2-aminoisobutyric acid)] were placed in positions 7, 10 and 13 to modulate side-chain density and helix stability [25]. Aib and Acp in particular are reported to stabilize the helical structure efficiently, whereas the capacity of Dpg and Deg to do this is less certain [25,26].

In the series P2, P7–P9 (Table 1, Figure 2), the length of the charged or polar residue side chains was varied by interchanging the cationic residues Lys, Orn, Dab (2,4-diaminobutyric acid) and Dap (2,3-diaminopropionic acid) and the neutral polar residues Gln, Hse (homoserine) and Ser while keeping the hydrophobic sector constant.

A longitudinal hydrophobicity gradient was introduced by systematically decreasing linear and branched aliphatic residue side-chain sizes along the helical axis, in both N- to C-terminal (P10) and C- to N-terminal (P11) directions (see Table 1 and Figure 1).

It should be stressed that an attempt was made to vary the parameters as far as possible independent of each other. Thus the charge and size were kept constant, as were the residue distribution (in terms of polar/hydrophobic residues), thus suggesting that some parameters that can markedly affect membrane interaction [19], such as the angle subtended by the hydrophobic and polar

sectors and therefore their surface area, are also fairly constant. However, these to some extent do depend on the spread resulting from side-chain lengths and also assume complete helical structuring. In some cases, and in particular for peptides with a lower helix-forming propensity in TFE (trifluoroethanol) or SDS, a more significant deviation may occur [27]. This helix-forming propensity should however be distinguished from the helical content of the peptide when it is membrane-bound. It is well known that the membrane environment very strongly induces the helical conformation, imposing it even on diastereomeric peptides [28].

Physicochemical and structural properties

As expected, variations in the polar face (P2, P7–P9) have a less marked effect on the overall hydrophobicity of the model peptides compared with variations of the hydrophobic face (P2–P6). Thus P5 has the lowest hydrophobicity compared with P1 (-2.65 versus -0.06), due to its shallow hydrophobic sector, whereas P3 has the highest (0.09), followed by P6 (0.04) due to the high density of large aliphatic side chains in their hydrophobic face (Figure 1, Table 2).

The propensity of the peptides to assume a helical structure in the presence of the helix-stabilizing solvent TFE or membrane mimicking SDS micelles, as determined by CD (Table 2, and Figure S1 at http://www.BiochemJ.org/bj/390/bj3900177add.htm), depended on both the overall properties of the hydrophobic sector and the presence of α-branched residues. A shallow hydrophobic face correlated with a reduced helix-forming propensity (P4 and P5 in Table 2), and this was also the case for the peptides with a depth gradient in this face (P10 and P11 in Table 2, and Figure S1 at http://www.BiochemJ.org/bj/390/bj3900177add.htm), i.e. where one or other of the extremities is shallow. P3 showed the most marked increase in conformational stability in all environments, due to the presence of the cyclic, α-branched Acp residues, being the only peptide to structure significantly also in aqueous solution. Aib also aided structuring, but to a lesser extent (e.g. P2 versus P1), whereas Dpg (P6) did not, in agreement with literature reports [25], probably because of steric reasons. The characteristics of the polar sector also affected structuring (Table 2), but in a manner that did not correlate with its depth, as P2 showed a reproducibly lower helix content ($\sim$60 %) compared with the peptides with a deeper (P7) or shallower (P8 and P9) polar face. The reason for this is not clear. The reduced capacity of P9 to structure in the presence of SDS micelles with respect to TFE can be interpreted as being due to its reduced capacity to penetrate into the lipid layer via the snorkel effect.

A clear correlation was observed between RP-HPLC retention times and both the hydrophobic and polar face depths (P1 > P2 > P4 > P5 and P7 > P2 > P8 > P9). In this case, the C_{18} layer can also be considered as a simple model for the membrane lipid environment [29], and the first series confirms the importance of hydrophobic interactions, whereas in the second series, retention times decrease with decreasing polar side-chain size, confirming the snorkel effect. In this respect, the optimized structuring and hydrophobicity of P3 resulted in the highest retention time, but the latter property seems to be the key parameter, as shown by the high retention time of P6 also, which is almost as hydrophobic, but has a lower propensity for helical structuring. In fact, this experiment exemplifies the interconnection between structuring and the effective hydrophobicity. The global hydrophobicity determines the initial interaction with the lipid layer, inducing structuring and thus the formation of a hydrophobic surface. This hydrophobic surface area then sinks into the lipid layer, in a manner that depends on the side-chain size, resulting in a further stabilization of the structure and increased interaction.

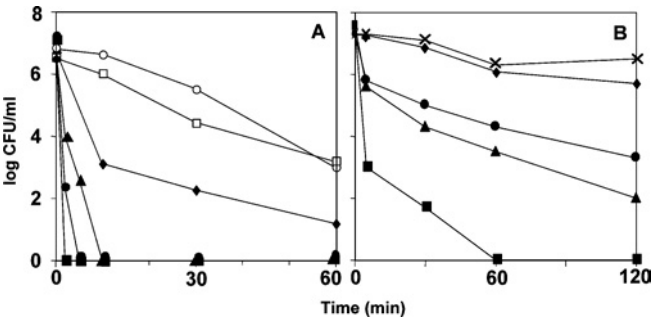

Figure 3 Kinetics of bacterial killing for selected model peptides

Colony counts for *E. coli* ML-35 (**A**) and *Staph. aureus* 710A (**B**) exposed to P2 (◆, 8 μM), P3 (■, 8 μM and □, 0.5 μM), P6 (▲, 8 μM), P7 (●, 8 μM and ○, 0.5 μM) or P9 (× , 8 μM) in PBS.

Biological activity

Although all the reported peptides have a similar size, charge, and hydrophobic/polar residue distribution, the structural variations described above had a marked effect on the *in vitro* antimicrobial potency, in terms of MIC. A homogeneously shallow hydrophobic face (aliphatic side chains of two carbon atoms or less, P4 and P5) effectively knocked out activity against all the standard microbial strains used (Table 2). The presence of a depth gradient, where only one end of this face is shallow (P10 and P11), also reduced potency and restricted the spectrum of activity. A limited number of shorter side-chain residues (e.g. three out of eight in P2 or P7) was instead well tolerated, as these peptides showed a potent and broad spectrum activity. Polar sector characteristics also had a discernible, albeit less marked, effect on the antimicrobial potency (see P2, P7–P9, Table 2), supporting a role for the snorkel effect in the microbial inactivation mechanism.

Unexpectedly, P3, which has optimized hydrophobicity, amphipathicity and helix stability, showed a significantly reduced potency. This was however found to be quite medium-dependent, so that activity compared favourably with that of the peptides P1 or P2 in reduced medium [e.g. 5 % (v/v) MH broth in PBS; Table 2, values in parentheses], and in some batches of full strength MH broth, but not in others. An explanation for this is that this peptide probably aggregates and/or interacts more strongly with components of the medium, so as to reduce its activity in these assays. Synthetic peptides based on a hybrid cecropin-melittin sequence, in which a stabilized helical structure was imposed by the formation of lactam bridges between Glu^{i} and Lys^{i+4} side chains in the polar sector, also showed reduced activity [30].

The killing kinetics for some of the peptides against reference *Staph. aureus* and *E. coli* strains is shown in Figure 3. Trends are similar for both microorganisms, although for any given peptide, the killing of the Gram-positive microorganisms was considerably slower. P3, with its optimized physicochemical properties and structural stability, was the most efficient at killing both microorganisms, under the conditions of this assay. Furthermore, the significantly faster killing kinetics of P7 with respect to peptides with a shallower polar sector indicates that insertion depth, via the snorkel effect, affects the killing mechanism. P3 and P7 retained a significant killing capacity towards *E. coli* also at reduced concentrations (Figure 3A).

The haemolytic activity of the peptides, a measure of their selectivity for microbial cells, follows the same trend (P6 > P1 = P2 > P4 > P5 and P7 > P2 = P8 > P9) as antimicrobial activity, consistent with a membranolytic mechanism for both types of cells, but is generally quite moderate at 10 μM, a concentration

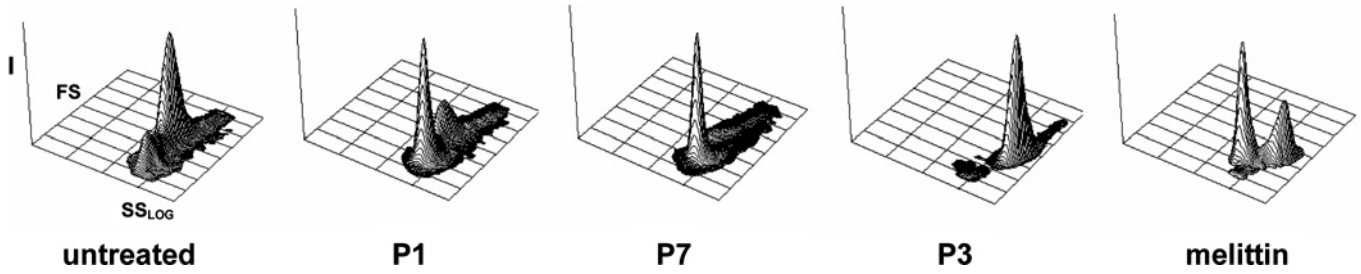

Figure 4 Three-dimensional flow cytometric contour-plot analysis of mouse lymphocytes treated with selected model peptides and the bee toxin melittin

FS (*y*-axis) is an indicator of size and SS (90° scattering, SS_{LOG}, *x*-axis) is an indicator of granularity. The *z*-axis represents the cellular population intensity. Cells were exposed to 10 μM peptide in PBS.

at which most peptides are antimicrobially active *in vitro*. Thus host cell disruption is also affected by both the hydrophobic face depth and the snorkel effect. In contrast with the antimicrobial activity, however, the presence of an oblique hydrophobicity gradient (P10 and P11) seems to favour haemolytic activity. The crucial factor appears to be the conformational stability, with P3 showing a particularly high haemolytic activity already at 10 μM, confirming previously reported observations [15].

Mode of action

Several different techniques were used to probe the capacity of the model peptides to interact with and permeabilize biological membranes, in real or model systems. The kinetics of bacterial membrane permeabilization of both the outer and cytoplasmic membranes of *E. coli* ML-35 (Table 2, and Figure S2 at http://www.BiochemJ.org/bj/390/bj3900177add.htm) was fastest for the highly structured and hydrophobic P3, followed by the less structured but equally hydrophobic P6. Decreasing the depth of the polar face (e.g. P9) significantly reduced the capacity to rapidly permeabilize either membrane, whereas reducing the depth of the hydrophobic face (P4 and P5) effectively abolished it. Curiously, P11 with an N $\rightarrow$ C oblique hydrophobicity gradient was more effective in permeabilizing both membranes than P10, with the gradient in the opposite direction. For any given peptide, permeabilization of the *Staph. aureus* cytoplasmic membrane was slower than that of the Gram-negative bacterium, in line with the killing kinetics. In this case, P6 was by far the most effective peptide, whereas reduction of the hydrophobic face depth drastically reduced the activity also in the partial case of the peptides with a hydrophobicity gradient (P4, P5, P10 and P11). Conversely, the effect of polar sector depth is less marked compared with that for *E. coli*. Taken together, these results indicate that the mechanism of membrane lysis by the peptides for the two microorganisms has some common features, but differed somewhat in other respects, possibly also due to different membrane phospholipid compositions (PE is predominant in *E. coli* whereas PG is in *Staph. aureus*).

Permeabilization of mouse lymphocytes to PI was determined for P1, P3 and P7, using flow cytometric methods (Figure 4). In the absence of peptides, a homogeneous population of non-fluorescing, undamaged cells dominates. In the presence of 10 μM P1 or P7, a second population of damaged and permeable cells [high fluorescence, decreased FS (forward scattering)] becomes dominant, in line with a previous observation, probably indicating a necrotic inactivation of cells [15]. P3 acts via a different mechanism, the massive permeabilization being accompanied by increased side scatter, indicating a more granular morphology. As the highly haemolytic activity of this peptide was reminiscent of that of the α-helical bee venom toxin melittin, this was also tested under the same conditions, with an intermediate result, both decreased-FS and increased-SS (side scattering) populations being observed.

The behaviour of P3 was studied in more detail, comparing flow cytometric and SEM results (Figure 5). At a low concentration ($\leqslant 1$ μM), it appears to behave like the other peptides (P1 or P7), inducing a decreased-FS population (Figures 5B and 5F), so that cells appear to shrink and become highly permeable to PI, although little apparent membrane damage is evident by SEM (Figure 5J). At a higher concentration (10 μM), only the highly permeable, increased-SS population is evident (Figures 5C and 5G), corresponding to a highly granular morphology as observed by SEM (Figure 5K). Melittin (Figures 5D, 5H and 5L) again showed an intermediate behaviour.

The different behaviours of P3 towards both host cells and microbial cells with respect to that of the other peptides from this series, prompted us to investigate interactions with model membranes using SPR. The sensograms for P3 and P1, interacting with anionic PE/PG or zwitterionic PC/cholesterol model membranes, are compared in Figure 6, and it is immediately apparent that they behave differently. P1 binds more efficiently to PE/PG than PC/cholesterol, but also washes out more easily. P3 binds with a similar efficiency to PE/PG and PC/cholesterol but dissociates significantly more slowly than P1, with a significant portion of the peptide remaining bound to the PC/cholesterol membrane on washing, in the timescale of the experiment.

The average values for the rate constants obtained after fitting an integrated rate equation for a two-state reaction model directly to the observed sensograms [23] are listed in Table 3, along with the estimated affinity constant values for the two steps (K_1 represents the binding to the surface and K_2 further insertion) implicit in this model, and lead to several significant observations. First, P3 has higher affinity than P1 towards PE/PG bilayers as a result of the first binding step ($K_1 = 2 \times 10^5$ and 5.5×10^4 M^{-1} respectively), with an approx. 20-fold faster binding (k_{a1}) and approx. 2-fold slower dissociation (k_{d1}) than P1. The binding rate constants to PE/PG for the two peptides in the second (insertion) step are instead similar (Table 3). Conversely, P3 and P1 have similar affinities towards PC/cholesterol in the first binding step ($K_1 \sim 1.7 \times 10^5$ M^{-1}), but P3 inserts into PC/cholesterol approx. 10-fold better in the second step. Thus P3, which is more active than P1 against bacterial cells under appropriate conditions, binds better to PE/PG bilayers principally due to the first surface binding process. On the other hand, the increased cytotoxic activity of P3 towards host cells may be derived from the second membrane

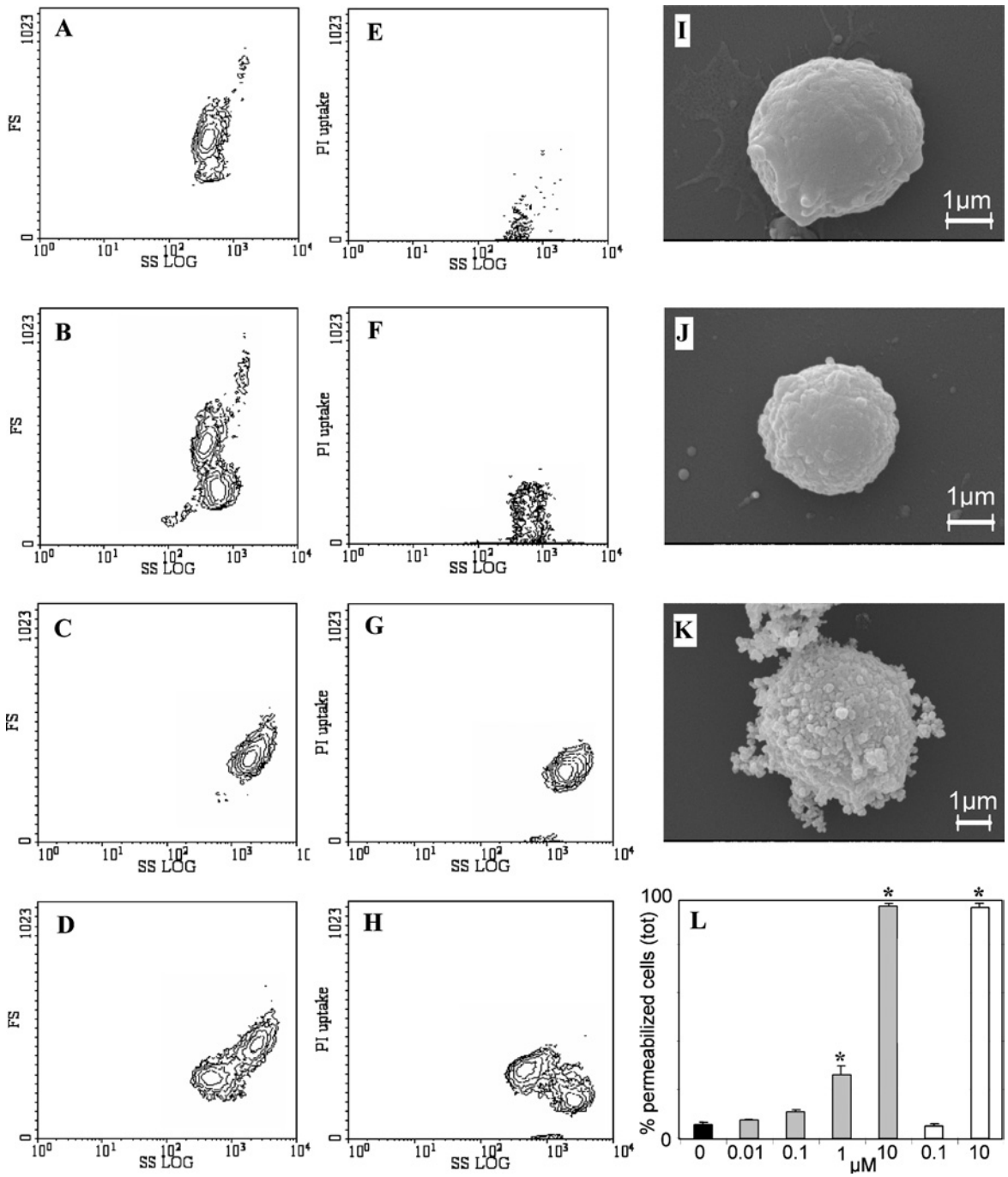

Figure 5 Effect of P3 on mouse lymphocytes determined by flow cytometry and SEM

The flow cytometric contour-plot analysis shows FS (**A**–**D**) and PI uptake (**E**–**H**) versus SS, at increasing peptide concentration. Scanning electron micrographs (**I**–**K**) show leucocytes treated with peptide at the same concentrations. (**A**, **E**, **I**) Blank control, (**B**, **F**, **J**) 1 μM P3, (**C**, **G**, **K**) 10 μM P3 and (**D**, **H**) 10 μM melittin. The histogram (**L**) shows percentage of PI uptake for the blank control (black), and at the different concentrations of P3 (grey) or melittin (white). Results shown are the means $\pm$ S.E.M. for five samples/group. $^*P < 0.05$, statistically different from control (ANOVA, Student–Newman–Keuls post test).

insertion step. SPR experiments performed with melittin under the same conditions indicate that it behaves similar to P3 with regard to PC/cholesterol in the second insertion step (Table 3), although showing a higher affinity in the first binding step. Thus both SPR experiments on model membranes and flow cytometric experiments on host cells indicate that P3 behaves more like the bee venom, melittin, a model of a non-cell-selective peptide, whereas P1 behaves more like canonical helical AMPs such as magainin that are bacteria-selective [31].

Spectrum of activity and therapeutic potential

For a more extensive appraisal of the potential of the described peptides as anti-infective agents, selected peptides were tested against a wider range of pathogenic indicator strains, some of which multiply resistant to clinically used antibiotics. For this purpose, an optimized and standardized version of the MIC assay was used [32], in which an MIC value of 4 or less was considered to confirm a useful antimicrobial activity (Figure 7).

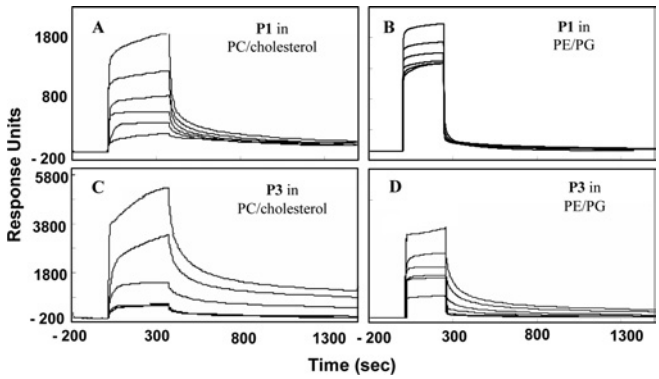

Figure 6 SPR sensograms for the binding of P1 and P3 with model membranes

(**A**) P1 in PC/cholesterol (10:1, w/w) and (**B**) P1 in PE/PG (7:3, w/w) lipid bilayers (using the L1 chip). (**C**) P3 in PC/cholesterol (10:1) and (**D**) P3 in PE/PG (7:3) lipid bilayers. Traces with increasing intensities correspond to peptide concentrations of 0.45, 0.9, 1.8, 3.6, 7.0 and 15 μM.

While the parent peptide, P1, already showed an acceptable overall antibacterial activity, increasing the helix propensity in P2 extended this to yeasts, whereas the presence of a deeper polar face in P7 appeared to improve activity towards Gram-positive microorganisms in particular. The medium dependence of P3's activity instead reduced its effectiveness in this assay. Overall, the generally broad spectrum of activity of P2 and especially of P7 against both Gram-positive and Gram-negative pathogens, including several multiple antibiotic-resistant strains, combined with their relatively small size and simplicity, makes them suitable as lead compounds for the development of novel anti-infective agents.

DISCUSSION

The initial electrostatic interaction of AMPs with the negative cell surface of bacteria is widely believed to be the first step in their mechanism of action and may not require structuring. However, the efficiency of the second step, which is the transition through the cell wall and partitioning into the membrane, depends on size, charge and the structural properties of the peptides. Here, by using a set of model peptides with rationally designed systematic variations in three key structural characteristics: hydrophobic sector depth, polar sector depth and propensity for helical structuring, while keeping other parameters such as size, charge and hydrophobic/polar residue distribution constant, we have been able to probe the interaction of helical AMPs with membranes in both model membranes and cellular systems.

Permeabilization and killing kinetics are consistently slower for Gram-positive with respect to Gram-negative bacteria (Figure 3, and Figure S2 at http://www.BiochemJ.org/bj/390/bj3900177add.htm.) [12–14], so that the thick, polar peptidoglycan layer of the former may be of greater impedance than the outer membrane of the latter, which is an anisotropic layer with a lipid core. Breaching of the outer membrane in *E. coli* is in fact quite rapid, as subsequent permeabilization of the cytoplasmic membrane is hardly delayed (Figure S2 at http://www.BiochemJ.org/bj/390/bj3900177add.htm.), and requires hydrophobic interaction of peptides with the lipid core as indicated by the reduced ability of P4 and P5 to effect its permeabilization (see also [33,34]).

Once the peptides reach the negatively charged cytoplasmic membrane, they lie parallel to the surface of the outer leaflet, according to what has been termed the 'carpet model', where they accumulate until a threshold concentration is reached [7,9,35,36]. These processes have been variously proposed to result in a purely detergent-like disruption of the membrane [9], in more well-defined membrane apertures usually described as 'toroidal', 'wormhole' or 'dynamic peptide–lipid supramolecular' pores [35,37,38], or from amorphous areas of increased permeability termed 'aggregate channels' [11]. The formation of membrane spanning classical 'barrel stave' pores instead is unlikely [35].

Membrane insertion and dependence on helix stability

A transition of the peptide chain to a helical conformation is required to form the amphipathic structure. Our results indicate that this process depends markedly on side-chain size, requiring a threshold number of residues with chains of three or more carbon atoms to be present and spread throughout the entire hydrophobic face. Shorter residues can be interspersed among these, but clustering of larger residues at one extremity of the chain is ineffective for bactericidal activity.

Membrane insertion stabilizes the helix throughout its length and decreases main-chain polarity by promoting more extensive H-bonding [39]. This allows a deeper penetration into the bilayer and it is then the length of side chains on the polar face, which are aliphatic except for the head-groups, that determines the final degree of insertion by what is termed the snorkel effect. We could observe how this modulates the strength of interaction even in a very simple model for the lipid layer provided by the C_{18} phase in RP-HPLC (see above, Table 2), and how it affects antimicrobial potency. This snorkel effect furthermore seems to be a common requirement for permeabilization of both bacterial and eukaryotic membranes.

Structuring is required for, but also depends on, hydrophobic interactions with the membrane. The intrinsic propensity of a peptide for assuming a helical conformation should thus affect its capacity to permeabilize biological membranes. We have reported

Table 3 Association (k_{a1} and k_{a2}) and dissociation (k_{d1} and k_{d2}) rate constants in bilayers determined by SPR with numerical integration using the two-state reaction model

The affinity constants K_1 and K_2 are for the first ($K_1 = k_{a1}/k_{d1}$) and second ($K_2 = k_{a2}/k_{d2}$) steps respectively, and the affinity constant (K) determined as $(k_{a1}/k_{d1}) \times (k_{a2}/k_{d2})$ is for the complete binding process.

Peptide	Lipid	k_{a1} ($M^{-1} \cdot s^{-1}$)	$k_{d1} \times 10^6$ (s^{-1})	$K_1 \times 10^{-4}$ (M^{-1})	$k_{a2} \times 10^3$ (s^{-1})	$k_{d2} \times 10^3$ (s^{-1})	K_2	$K \times 10^{-4}$ (M^{-1})
P1	PC/cholesterol	1.2 (±0.06)	6 (±0.9)	17.1	2 (±0.1)	0.9 (±0.04)	1.8	30.1 (±1)
	PE/PG	1.1 (±0.03)	20 (±0.09)	5.5	2 (±0.4)	0.7 (±0.02)	3.1	17.1 (±0.8)
P3	PC/cholesterol	1.1 (±0.06)	5 (±0.7)	16.6	15 (±1)	0.8 (±0.1)	22	365 (±20)
	PE/PG	20.0 (±1)	10 (±0.4)	20.0	2 (±0.1)	1 (±0.2)	1.7	34 (±2)
Melittin	PC/cholesterol	19.0 (±1.5)	500 (±40)	3.8	410 (±40)	25 (±2)	16.5	62.3 (±3.4)
	PE/PG	15.5 (±1.1)	400 (±30)	3.9	115 (±10)	16 (±1)	7.2	27.9 (±1.7)

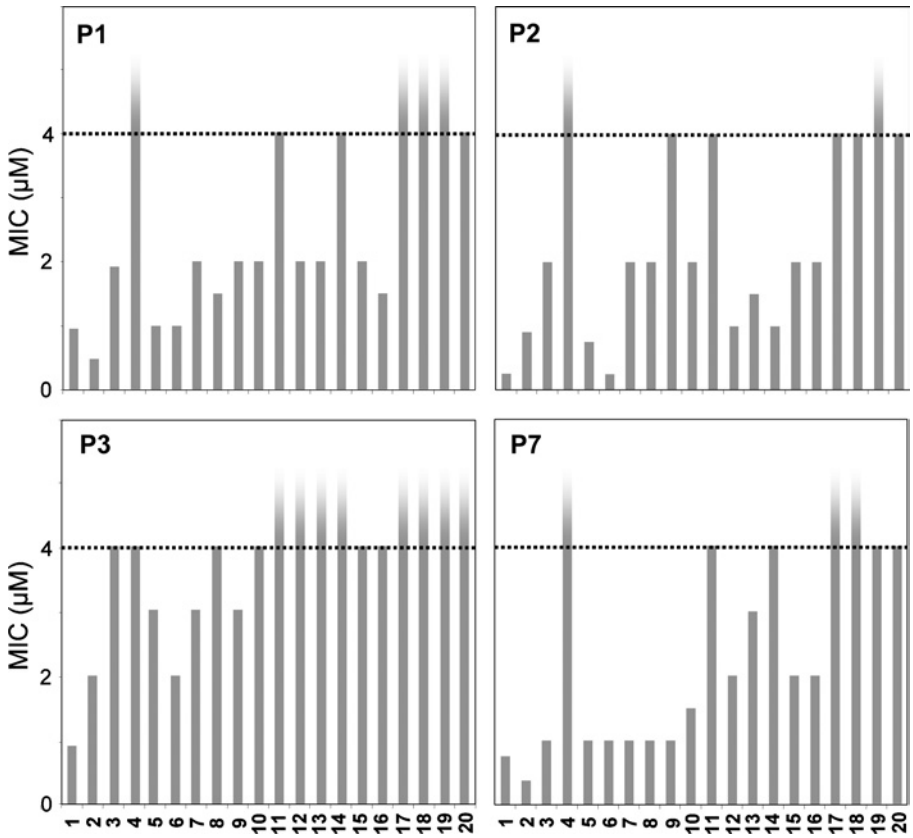

Figure 7 Spectrum of antimicrobial activity of selected model peptides

The tested indicator strains were two standard laboratory strains as well as 18 clinical isolates with varying antibiotic susceptibility patterns: (1) *Staphylococcus simulans*; (2) *Micrococcus luteus*; (3) *Enterococcus* spp., I-11305b; (4) *Enterococcus* spp., I-11054; (5) KNS, I-10925; (6) MRSE, LT1324; (7) *Staph. aureus*, 5185; (8) *Staph. aureus*, I-11574; (9) MRSA, LT1338; (10) MRSA, LT1334; (11) *Citrobacter freundii*, I-11090; (12) *Klebsiella pneumoniae*, I-10910; (13) *E. coli*, I-11276b; (14) *E. coli*, O-12592; (15) *Stenotrophomonas maltophila*, O-16451; (16) *S. maltophila*, I-10717; (17) *Pseudomonas aeruginosa*, 4991; (18) *Ps. aeruginosa*, I-10968; (19) *Candida albicans*, I-11301; (20) *C. albicans*, I-11134. An MIC value of 4 was arbitrarily chosen as the threshold value for potency. All MIC values above 4 are not given.

previously that it particularly affects host cell cytotoxicity [15] and it is confirmed here with the highly cytotoxic P3, which has a stable helical structure already in the bulk phase. At the other extreme, previously reported diastereomeric peptides, with a low helix-forming propensity, maintained a reasonable antimicrobial activity associated with a remarkably low cytotoxicity [32,40].

SPR studies on model membranes, comparing P3 with P1, which has quite similar physicochemical properties but is unstructured in the bulk phase (Table 2), indicated that the initial interaction of P3 with the anionic PE/PG membrane (bacterial model) is much faster than P1, while subsequent insertion into the membrane is comparable. An explanation may be that being prestructured and probably aggregated in solution, P3 displays an increased charge/density ratio and is thus subject to a stronger electrostatic interaction with the anionic membrane surface (step 1). Membrane insertion leads to structuring of P1 and probably results in the disaggregation of P3 [41] so that they behave similarly in the second step. Conversely, the initial interaction with a model eukaryotic membrane (PC/cholesterol), which is electrically neutral, does not markedly differ for the two peptides, irrespective of their structural characteristics, whereas there is a considerable difference in the subsequent insertion step. The preformed P3 helical system binds to PC/cholesterol over 10-fold better than P1, probably because it inserts deeper into the inner leaflet. In contrast, there is only a 2-fold difference in the binding of P3 and P1 to negatively charged PE/PG membranes, indicating that the inner leaflet contributes only slightly to their binding to PE/PG bilayers. Furthermore, as the presence of an oblique hydrophobicity gradient [42] favours haemolytic activity but not bacterial inactivation, it is possible that it also affects the second step (insertion) in eukaryotic membranes. Overall, the tendency to prestructure/aggregate in solution leads to a shift in the mode of action that correlates with an increased toxicity towards host cells, and may provide some insights into the mechanisms underlying it.

Types of mebranolytic activity

From the above considerations, α-helical peptides such as those studied here can be divided into two types, (i) AMPs which we could term as canonical α-helical AMPs that are more bacteria-selective and (ii) aggregation-prone α-helical AMPs that are not cell-selective and their behaviour used to interpret that of natural peptides. P1 or P7 can be considered as simplified analogues of canonical α-helical AMPs such as the much studied amphibian magainin [2,7,9,33,38], which has a similar size (22 residues) and charge (+5), as well as many others [8], which are unstructured in bulk solution. P3 instead behaves more like the bee toxin melittin [2,31,34,35,37] or like the human cathelicidin-derived α-helical peptide LL-37. Indeed, LL-37, like P3, has a tendency to structure and aggregate in bulk solution under certain conditions [43], it is quite cytotoxic [41], and its cytotoxicity and antimicrobial activities are quite medium sensitive [44].

The peptides P1 or P7, like magainin, show a relatively moderate cytotoxicity towards animal cells. They permeabilize lymphocyte membranes leading to a necrotic effect, characterized by increased PI uptake and decreased FS in flow cytometric experiments (Figure 5). This correlates with the propensity for helical structuring (see also [12,15]). For P3, a markedly increased PI uptake is instead associated with a shift in the SS parameter that indicates increased granularity, corresponds to a highly pocked surface in SEM (Figure 5) and is consistent with a different type of membrane damage. An increased log SS has also been described for melittin acting on the HMy2 human lymphoblastoid cell line [45], and was interpreted in terms of the formation of lipid vesicles on the cell membrane or intracellularly, which is compatible with our observations. P3 is more cytotoxic than melittin, which shows an intermediate effect on lymphocytes at equivalent concentration, with both types of damaged cell populations being present. In fact, P3 switches from one mode to the other in a concentration-dependent manner, which could indicate a two-stage mechanism, with one type of permeabilization leading to the other, but only for aggregation-prone peptides at higher concentrations. The aggregation-prone LL-37 also behaves in a quite similar manner (unpublished work). In this respect, it is possible that this type of peptide might access alternative mechanisms for membrane penetration, such as the 'sinking raft' model proposed by Pokorny and Almeida [46].

Interaction model

It has been widely reported that the presence of anionic phospholipids in bacterial membrane is a principal factor in determining AMP selectivity with respect to zwitterionic host cells, but this has been generally simply ascribed to increased attraction for these cationic molecules. Apart from promoting the initial docking, electrostatic interactions may play an important role also in the subsequent structuring/membrane insertion steps. Interaction with anionic head groups may help to dunk the peptides deeper into the membrane in accordance with the snorkel effect. Bulk phase structuring/aggregation affects the initial interaction with the anionic surface, as discussed above, but is probably eliminated by electrostatic interaction with the head groups [41], so that the final membrane-bound state is similar for canonical and aggregation-prone α-helical peptides. For membranes formed by zwitterionic phospholipids, the latter instead seem to have a definite advantage. One explanation could be that the entropy loss on the transition from random coil to helix, on membrane insertion, might have a greater effect on partitioning in the absence of electrostatic interactions. Another could be that the particular lytic mechanism for membranes formed by zwitterionic phospholipids benefits from aggregation, as has been proposed for LL-37 [41]. It is not however due to reduced partitioning into outer-wall components such as sialic acids, as has been suggested for melittin [47], as we observed a differential interaction with naked model membrane systems.

Finally, our results indicate that the physical interaction of the peptides with the membrane, as proposed by the various mechanisms that can be included in the carpet model, is the principal factor leading to cellular inactivation. However, this does not exclude that other effects involving the bacterial cell wall and membrane, such as activation of autolytic enzymes in bacteria [48], or of endogenous phospholipases in host cells [49] by the AMPs, or interactions of the AMPs with internal targets once the membrane is breached, could also have important accessory roles. Nevertheless, the considerations presented in the this study are not only useful to understand better the behaviour of natural α-helical AMPs and toxins, but also furnish a framework for the design of synthetic AMPs with optimized activity/selectivity profiles for possible biomedical applications.

This work was supported by grants from the Italian Ministry of Universities and Scientific Research (PRIN 2003), and from a Friuli-Venezia Giulia regional grant. I.Z. and U.P. have been supported by a grant from the V Framework EU PANAD project QLK2-CT-2000-00411. H.-G.S. acknowledges financial support for antimicrobial peptide research from the Deutsche Forschungsgemeinschaft. The free-of-charge availability of the flow cytometry facility of the Fondazione Callerio ONLUS is also gratefully acknowledged.

REFERENCES

1 Sargent, D. F. and Schwyzer, R. (1986) Membrane lipid phase as catalyst for peptide-receptor interactions. Proc. Natl. Acad. Sci. U.S.A. **83**, 5774–5778
2 Kourie, J. I. and Shorthouse, A. A. (2000) Properties of cytotoxic peptide-formed ion channels. Am. J. Physiol. Cell Physiol. **278**, C1063–C1087
3 Zasloff, M. (2002) Antimicrobial peptides in health and disease. N. Engl. J. Med. **347**, 1199–1200
4 Frankel, A. E., Neville, D. M., Bugge, T. A., Kreitman, R. J. and Leppla, S. H. (2003) Immunotoxin therapy of hematologic malignancies. Semin. Oncol. **30**, 545–557
5 Papo, N. and Shai, Y. (2003) New lytic peptides based on the D,L-amphipathic helix motif preferentially kill tumor cells compared to normal cells. Biochemistry **42**, 9346–9354
6 Zasloff, M. (2002) Antimicrobial peptides of multicellular organisms. Nature (London) **415**, 389–395
7 Shai, Y. (2002) Mode of action of membrane active antimicrobial peptides. Biopolymers **66**, 236–248
8 Tossi, A., Sandri, L. and Giangaspero, A. (2000) Amphipathic, alpha-helical antimicrobial peptides. Biopolymers **55**, 4–30
9 Oren, Z. and Shai, Y. (1998) Mode of action of linear amphipathic alpha-helical antimicrobial peptides. Biopolymers **47**, 451–463
10 Matsuzaki, K. (1998) Magainins as paradigm for the mode of action of pore forming polypeptides. Biochim. Biophys. Acta **1376**, 391–400
11 Hancock, R. E. and Chapple, D. S. (1999) Peptide antibiotics. Antimicrob. Agents Chemother. **43**, 1317–1323
12 Tossi, A., Tarantino, C. and Romeo, D. (1997) Design of synthetic antimicrobial peptides based on sequence analogy and amphipathicity. Eur. J. Biochem. **250**, 549–558
13 Giangaspero, A., Sandri, L. and Tossi, A. (2001) Amphipathic alpha helical antimicrobial peptides. Eur. J. Biochem. **268**, 5589–5600
14 Tiozzo, E., Rocco, G., Tossi, A. and Romeo, D. (1998) Wide-spectrum antibiotic activity of synthetic, amphipathic peptides. Biochem. Biophys. Res. Commun. **249**, 202–206
15 Pacor, S., Giangaspero, A., Bacac, M., Sava, G. and Tossi, A. (2002) Analysis of the cytotoxicity of synthetic antimicrobial peptides on mouse leucocytes: implications for systemic use. J. Antimicrob. Chemother. **50**, 339–348
16 Powers, J. P. and Hancock, R. E. (2003) The relationship between peptide structure and antibacterial activity. Peptides **24**, 1681–1691
17 Epand, R. M., Shai, Y., Segrest, J. P. and Anantharamaiah, G. M. (1995) Mechanisms for the modulation of membrane bilayer properties by amphipathic helical peptides. Biopolymers **37**, 319–338
18 Dathe, M. and Wieprecht, T. (1999) Structural features of helical antimicrobial peptides: their potential to modulate activity on model membranes and biological cells. Biochim. Biophys. Acta **1462**, 71–87
19 Dathe, M., Meyer, J., Beyermann, M., Maul, B., Hoischen, C. and Bienert, M. (2002) General aspects of peptide selectivity towards lipid bilayers and cell membranes studied by variation of the structural parameters of amphipathic helical model peptides. Biochim. Biophys. Acta **1558**, 171–186
20 Wieprecht, T., Dathe, M., Krause, E., Beyermann, M., Maloy, W. L., MacDonald, D. L. and Bienert, M. (1997) Modulation of membrane activity of amphipathic, antibacterial peptides by slight modifications of the hydrophobic moment. FEBS Lett. **417**, 135–140
21 Tossi, A., Sandri, L. and Giangaspero, A. (2002) New consensus hydrophobicity scale extended to non-proteinogenic amino acids. In Peptides 2002: Proceedings of the 27th European Peptide Symposium (Benedetti, E. and Pedone, C., eds.), pp. 416–417, Edizioni Ziino, Naples, Italy
22 Gazit, E., Lee, W. J., Brey, P. T. and Shai, Y. (1994) Mode of action of the antibacterial cecropin B2: a spectrofluorometric study. Biochemistry **33**, 10681–10692
23 Mozsolits, H., Wirth, H. J., Werkmeister, J. and Aguilar, M. I. (2001) Analysis of antimicrobial peptide interactions with hybrid bilayer membrane systems using surface plasmon resonance. Biochim. Biophys. Acta **1512**, 64–76
24 Zelezetsky, I., Pag, U., Antcheva, N., Sahl, H. G. and Tossi, A. (2005) Identification and optimization of an antimicrobial peptide from the ant venom toxin pilosulin. Arch. Biochem. Biophys. **434**, 358–364

25 Toniolo, C., Crisma, M., Formaggio, F. and Peggion, C. (2001) Control of peptide conformation by the Thorpe-Ingold effect (C alpha-tetrasubstitution). Biopolymers **60**, 396–419
26 Karle, I. L. (2001) Controls exerted by the Aib residue: helix formation and helix reversal. Biopolymers **60**, 351–365
27 Tachi, T., Epand, R. F., Epand, R. M. and Matsuzaki, K. (2002) Position-dependent hydrophobicity of the antimicrobial magainin peptide affects the mode of peptide-lipid interactions and selective toxicity. Biochemistry **41**, 10723–10731
28 Oren, Z. and Shai, Y. (2000) Cyclization of a cytolytic amphipathic alpha-helical peptide and its diastereomer: effect on structure, interaction with model membranes, and biological function. Biochemistry **39**, 6103–6114
29 Blondelle, S. E., Ostresh, J. M., Houghten, R. A. and Perez-Paya, E. (1995) Induced conformational states of amphipathic peptides in aqueous/lipid environments. Biophys. J. **68**, 351–359
30 Houston, Jr, M. E., Kondejewski, L. H., Karunaratne, D. N., Gough, M., Fidai, S., Hodges, R. S. and Hancock, R. E. (1998) Influence of preformed alpha-helix and alpha-helix induction on the activity of cationic antimicrobial peptides. J. Pept. Res. **52**, 81–88
31 Papo, N. and Shai, Y. (2003) Exploring peptide membrane interaction using surface plasmon resonance: differentiation between pore formation versus membrane disruption by lytic peptides. Biochemistry **42**, 458–466
32 Pag, U., Oedenkoven, M., Papo, N., Oren, Z., Shai, Y. and Sahl, H. G. (2004) *In vitro* activity and mode of action of diastereomeric antimicrobial peptides against bacterial clinical isolates. J. Antimicrob. Chemother. **53**, 230–239
33 Matsuzaki, K., Sugishita, K. and Miyajima, K. (1999) Interactions of an antimicrobial peptide, magainin 2, with lipopolysaccharide-containing liposomes as a model for outer membranes of gram-negative bacteria. FEBS Lett. **449**, 221–224
34 Ding, L., Yang, L., Weiss, T. M., Waring, A. J., Lehrer, R. I. and Huang, H. W. (2003) Interaction of antimicrobial peptides with lipopolysaccharides. Biochemistry **42**, 12251–12259
35 Yang, L., Harroun, T. A., Weiss, T. M., Ding, L. and Huang, H. W. (2001) Barrel-stave model or toroidal model? A case study on melittin pores. Biophys. J. **81**, 1475–1485
36 Huang, H. W. (2000) Action of antimicrobial peptides: two-state model. Biochemistry **39**, 8347–8352
37 Matsuzaki, K., Yoneyama, S. and Miyajima, K. (1997) Pore formation and translocation of melittin. Biophys. J. **73**, 831–838
38 Ludtke, S. J., He, K., Heller, W. T., Harroun, T. A., Yang, L. and Huang, H. W. (1996) Membrane pores induced by magainin. Biochemistry **35**, 13723–13728
39 Ladokhin, A. S. and White, S. H. (1999) Folding of amphipathic alpha-helices on membranes: energetics of helix formation by melittin. J. Mol. Biol. **285**, 1363–1369
40 Oren, Z. and Shai, Y. (1997) Selective lysis of bacteria but not mammalian cells by diastereomers of melittin: structure-function study. Biochemistry **36**, 1826–1835
41 Oren, Z., Lerman, J. C., Gudmundsson, G. H., Agerberth, B. and Shai, Y. (1999) Structure and organization of the human antimicrobial peptide LL-37 in phospholipid membranes: relevance to the molecular basis for its non-cell-selective activity. Biochem. J. **341**, 501–513
42 Brasseur, R., Pillot, T., Lins, L., Vandekerckhove, J. and Rosseneu, M. (1997) Peptides in membranes: tipping the balance of membrane stability. Trends Biochem. Sci. **22**, 167–171
43 Johansson, J., Gudmundsson, G. H., Rottenberg, M. E., Berndt, K. D. and Agerberth, B. (1998) Conformation-dependent antibacterial activity of the naturally occurring human peptide LL-37. J. Biol. Chem. **273**, 3718–3724
44 Turner, J., Cho, Y., Dinh, N. N., Waring, A. J. and Lehrer, R. I. (1998) Activities of LL-37, a cathelin-associated antimicrobial peptide of human neutrophils. Antimicrob. Agents Chemother. **42**, 2206–2214
45 Weston, K. M., Alsalami, M. and Raison, R. L. (1994) Cell membrane changes induced by the cytolytic peptide, melittin, are detectable by 90 degrees laser scatter. Cytometry **15**, 141–147
46 Pokorny, A. and Almeida, P. F. (2004) Kinetics of dye efflux and lipid flip-flop induced by delta-lysin in phosphatidylcholine vesicles and the mechanism of graded release by amphipathic, alpha-helical peptides. Biochemistry **43**, 8846–8857
47 Perez-Paya, E., Houghten, R. A. and Blondelle, S. E. (1995) The role of amphipathicity in the folding, self-association and biological activity of multiple subunit small proteins. J. Biol. Chem. **270**, 1048–1056
48 Ginsburg, I. (2004) Bactericidal cationic peptides can also function as bacteriolysis-inducing agents mimicking beta-lactam antibiotics; it is enigmatic why this concept is consistently disregarded. Med. Hypotheses **62**, 367–374
49 Saini, S. S., Chopra, A. K. and Peterson, J. W. (1999) Melittin activates endogenous phospholipase D during cytolysis of human monocytic leukemia cells. Toxicon **37**, 1605–1619

Received 23 December 2004/5 April 2005; accepted 19 April 2005
Published as BJ Immediate Publication 19 April 2005, doi:10.1042/BJ20042138